TRANSACTIONS OF THE INSTITUTE OF AVIATION
217, p. 14-32 , Warsaw 2011

STATIC ANALYSIS OF PLASTIC LIMIT STATE OF THIN-WALLED BEAMS WITH OPEN CROSS-SECTIONS

Sebastian Gawłowski

Institute of Aviation

Abstract

The purpose of the paper is to explore the potential applications of the Vlasov theory to description of limit states of thin-walled beam sections. This study addresses static aspects only. The diagrams of stresses in the elastic range (predicted in accordance with the Vlasov theory) are utilised to obtain limit stress distributions.

The analysis covers several examples: torsion of I-section thin-walled beam, bending and torsion of I-section profile and bending with torsion of a channel profile. In the case of the second example, the engineering application is shown, too. The analysed diagrams of stresses in plastic hinges can be used to develop the interaction surfaces formulae, which enable us to assess the load capacity at collapse.

The finite element simulation (Abaqus) shows that values obtained by this method are lower estimations. Computation verifies the adequacy of limit stress distributions predicted by using of the Vlasov theory.

Keywords: thin-walled beam, the Vlasov theory, limit state, plastic hinge

INTRODUCTION

Underlying this study is the thin-walled beam theory formulated by Vlasov [1]. The graph theory is applied to simplify the thin-walled beam description. This new approach to the Vlasov theory is given by Piechnik [2]. The work [2] provides a complete solution to the problem of thin-walled beams mechanics in the elastic state. It explains why new elements were added to the Vlasov theory of thin-walled beams e.g. cross-sectional forces (stress resultants): bimoment, the Vlasov torsional moment, the Saint-Venant torsional moment and shows the normal and shear stress formulae, determined by sectorial co-ordinate and sectorial static moment, respectively. The instructions, most helpful in construction of plots of stress distribution in plastic hinges in the cases of thin-walled beams, are provided in [3], [4] and [5]. Additionally, the book [5] contains the steel profiles research data, which verify the considerations presented in this study.

The practical application of thus derived distributions of stresses in plastic hinges involves an algorithm, which enables the assessment of load capacity at collapse of thin-walled beams with open cross-sections. The algorithm is presented in more detail elsewhere, [6] and [7].

The [6] contribution compares the three sets of analytical, experimental and computational data. The latter are obtained using the shell finite element simulations (Abaqus)-[8].

This finite element method (FEM) program is a good tool for further studies.

The papers [9] and [10] introduce the „monitoring areas" concept.

In this approach the limit diagrams of normal and shear stresses can be assumed to be more accurate as shear stresses can linear vary across the thickness of thin-walled cross-section.

1. MAIN ASSUMPTIONS

The present analysis is based on the Vlasov theory, simplified by introduction of some elements of the graph theory. Thin-walled beams are described by co-ordinate systems: the global system *xyz* and the local one *xsn* - Fig. 1.

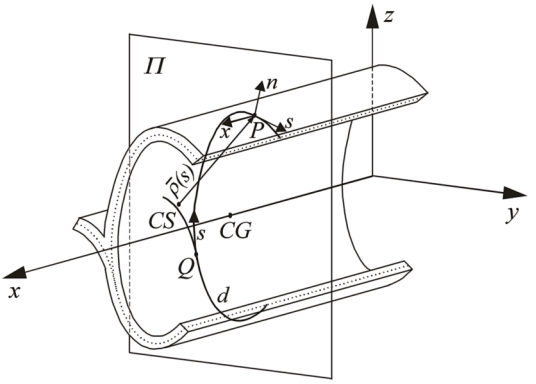

Fig. 1. The quantities used in the description of thin-walled beams in accordance with the Vlasov theory

The first system allows for defining the beam's geometry, whereas the components of stress and strain tensors are determined in the other one. The profile cross-section is reduced to the middle line (dendrite) *d*. Due to specific behaviour of thin-walled beams under the applied load (small stiffness and great warping of cross-sections), new quantities have to be introduced to create a right description of this group of structures.

On the profile cross-section plane-Fig. 1, several characteristic points are located. The point *CS* denotes the centre of shear. If applied forces pass the locus of *CS*, the thin-walled beam is only bent (without torsion). Generally, this point will not coincide with the centre of gravity *CG*, which happen in the case of solid (thick-walled) beams. The point *Q* is an origin of the natural parameter (co-ordinate) *s*. The location of *CS* and *Q* is found using a special procedure available in the Vlasov thin-walled beam description. The vector *ρ(s)* indicates the locus of any point *P* (for any parameter *s*) on the middle line *d*. As it is shown in Fig. 1, the local co-ordinate system *xsn* can be defined at any point of the *d* line. The axis *x* of the local system is parallel to the beam centre line-*x*-axis of the global system, whereas the axis *s* is tangent to the middle line and *n*-axis is perpendicular to *xs* plane. The global co-ordinate system axes *y* and *z* denote the principal directions of the cross-section.

The Vlasov theory introduces two important functions, which determine the distributions of normal and shear stresses on the cross-section: sectorial co-ordinate ω (s) and sectorial static moment S_ω (*s*). The first quantity defines normal stresses and is written as follows:

$$\omega(s) = \int_0^s \rho_n(s)\mathrm{d}s \tag{1}$$

The equation (1) represents a curvilinear integral over the middle line *d*, from the point *Q (s=0)* to any considered point *P*. The second function S_ω (*s*), is related to shear stresses and is obtained from (2).

$$S_\omega(s) = \int_s^{s_E} \omega(s)\delta(s)\mathrm{d}s \tag{2}$$

The integral in equation (2) is calculated from the given point to the end of an analysed leg of the cross-section. The symbol *δ(s)* denotes the cross-section thickness, which can vary along the middle line.

The solution to thin-walled beams mechanics problem is obtained by computing the *α(x)* (angle of beam rotation function) from the fundamental equation of the Vlasov theory (3).

$$\widetilde{E}I_\omega\alpha'''(x) - GI_s\alpha'(x) = -M_x^{CS}(x) \tag{3}$$

where:

$$\widetilde{E} = \frac{E}{1-\nu^2}, \quad G = \frac{E}{2(1+\nu)}$$

E-Young modulus, *ν*- Poisson ratio, I_ω-sectorial moment of inertia, I_S-torsional moment of inertia, $M_X(x)$ - function of total torsional moment (with respect to the centre of shear *CS*)

Apart from the Vlasov theory, normal and shear stresses diagrams in plastic hinges are constructed assuming that the material is elastic-perfectly-plastic. This model can be applied to simulations of behaviour of steel or aluminium - typical materials of thin-walled profiles. Under this assumption the stress distributions can be simplified using rectangles with one height for all parts of the cross-section. Obviously, the value of this height must not exceed the yield stress magnitude.

The presented algorithm for assessing load capacity at collapse is based on two assumptions. First, the Huber-Mises-Hencky yield criterion is used to describe the limit state. In the case of thin-walled beams this condition has the form (4).

$$\sigma_x^2 + 3\tau_{xs}^2 = \sigma_Y^2 \tag{4}$$

The symbols σ_X and τ_{XS} denote normal and shear stress, respectively, whereas σ_Y is a tensile yield stress value. Secondly, an assumption is made that the analysed profiles are these for which a plastic hinge appears before local instability. Accordingly, only a specific group of thin-walled beams with limited slenderness ratio of cross-sections legs will be considered.

2. TORSION OF I-SECTION THIN-WALLED BEAM

Let us consider cantilever I-section profile under torsion, as shown in Fig 2.

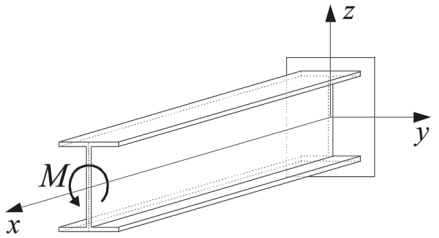

Fig. 2. The case of twisted concentrated moment applied to I-section cantilever thin-walled beam

If the solid beam theory is applied, only one cross-sectional force (torsional moment) will exist-related to shear stresses. However the fixed end of profile is a warping restraint, which causes also normal stresses to appear. This phenomenon is adequately described by Vlasov theory, which predicts the existence of new stress resultant (determined by normal stresses) - bimoment. The diagram of bimoment B_ω and the remaining nonzero cross-sectional forces, including: the Vlasov torsional moment M_ω and the Saint-Venant torsional moment M_S, are shown in Fig. 3.

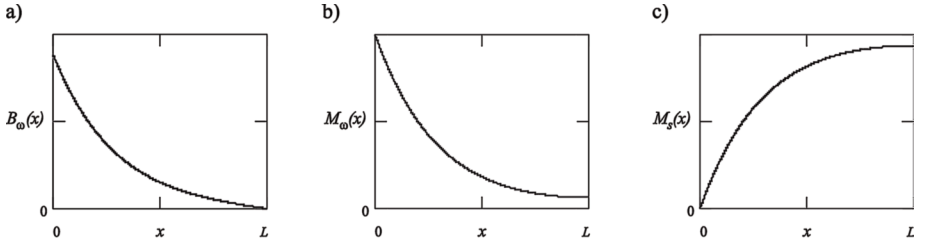

Fig. 3. The diagrams of cross-sectional forces in the considered problem: a) bimoment, b) the Vlasov torsional moment, c) the Saint-Venant torsional moment. The symbol *L* denotes a free end of beam abscissa (beam length)

The stress resultants distributions are determined by function $\alpha(x)$ and derived from equation (3). The suitable derivative relations have the forms:

$$\begin{aligned} B_\omega(x) &= \tilde{E} I_\omega \alpha''(x) \\ M_\omega(x) &= -\tilde{E} I_\omega \alpha'''(x) \\ M_s(x) &= G I_s \alpha'(x) \end{aligned} \tag{5}$$

The limit state of typical rolled steel cantilever I-section profile (investigated by Strelbicka et al.-[5]) was simulated using the finite element analysis (program Abaqus). The load applied to computational model of beam is equal to the limit magnitude, obtained experimetally. The loading way in FEM simulation, the experimental one (outlined in [5]) and that presented in Fig.2 are equivalent. The results (distributions of the Huber-Mises-Hencky reduced stress) for particular beam layers are shown in Fig.4.

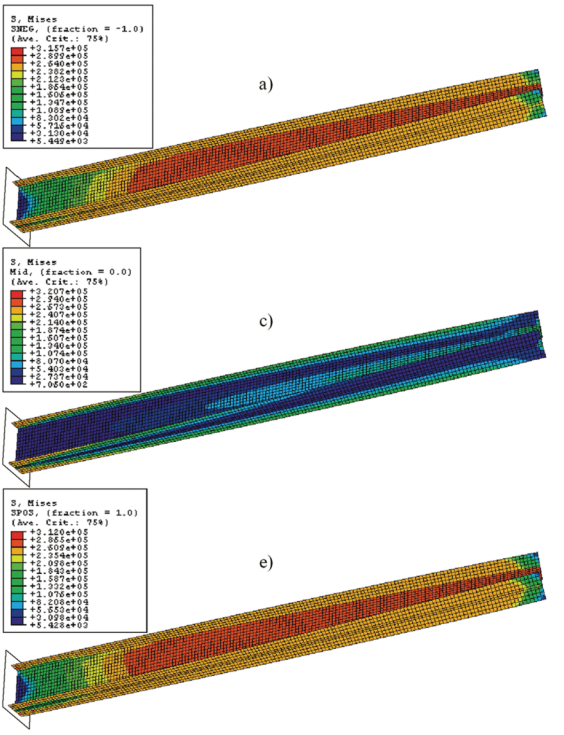

Fig. 4.

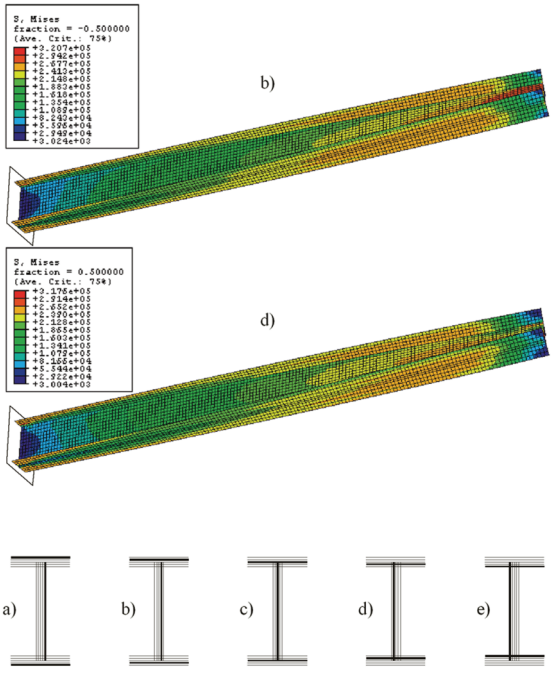

Fig. 4. The distributions of the Huber-Mises-Hencky reduced stress on different layers of profile. On the right bottom part of picture the views from free end of beam are presented.

Both, Fig. 3 and Fig. 4 illustrate the same issue-effort of thin-walled I-section cantilever beam.

In the case of FEM analysis, orange areas denote the spots where plastic yield process is active. In fact, the yield stress of beam web material is more than in the case of a flange, which is indicated by dark orange colour for the web.

In Fig. 4 two characteristic yield zones are apparent. The first one extends from the free end and involves ¾ of the profile. In this case the plastic yield is located in exterior layers, which suggests that it is generated when shear stresses achieves its limit level, because shear stresses have the biggest values at boundaries of the profile and become less in the interior (as in the case of the Saint-Venant torsion). The neutral points of shear stresses are located near the middle lines of cross-sections-Fig. 4c. The existence of these yield areas was predicted by the Vlasov theory. This form of beam effort is a consequence of great values of the Saint-Venant torsional moment, related to shear stresses-Fig. 3c, which are located in the same part of profile as the analysed yield zones.

The existence of second plastic yield area at the fixed end of the beam-Fig. 4, was clearly described by the Vlasov theory, too. The locus (near warping restraints) means that this yielding occurs when normal stresses achieves its limit value. This fact is confirmed by Fig. 3a

Fig. 4 shows also that plastic zones pass through all layers of profile flange, causing a plastic hinge to appear in this location. The specific form of plastic hinge (yielding of flanges and non-loaded web) - Fig. 4, is also observed during experiment-[5].

The construction of normal and shear stresses diagrams for a plastic hinge will be based on the elastic state analysis.

Fig. 3 shows, that limit stress distributions (cross-section x = 0) are determined only by two cross-sectional forces: Bω and Mω. The value of the Saint-Venant torsional moment at the fixed end equals zero.

Accordingly, stresses diagrams in plastic hinge are derived from formulas:

$$\sigma_x(s) = \frac{B_\omega}{I_\omega}\omega(s) \tag{6}$$

$$\tau_\omega(s) = -\frac{M_\omega S_\omega(s)}{I_\omega \delta} \tag{7}$$

The equation (6) shows that in the elastic state the normal stress *x* distribution over the cross-section is determined by sectorial co-ordinate, whereas in accordance with (7) the diagram of shear stresses (related to moment M_ω) is controlled by sectorial static moment (assuming that thickness is constant for each cross-section leg). Functions $\omega(s)$ and $S_\omega(s)$ for I-section are depicted in Fig. 5.

Fig. 5 (and Fig. 3c-zero value of M_s at the fixed beam end) show that the Vlasov theory predicts the existence of non-loaded web in the plastic hinge. This is shown by FEM analysis - Fig. 4, which is a good verification of the analytic limit state model of an I-section thin-walled beam.

Let us consider the sectorial co-ordinate diagram (normal stresses distribution in elastic range)-Fig. 5a. The plastic yield process begins when the maximum values of σ_x (at ends of flanges) achieve the limit magnitudes. Acting on the assumption that material is perfect (no hardening), the limit value must not be exceeded. The further loading generates the extension of stress limit areas along flanges to the web position. When the loading process is complete, the rectangular distributions of normal stresses appear-Fig. 6a. The applied load-Fig. 2 is responsible for asymmetry of this characteristic (the right top and left bottom parts of the section are tensioned whereas the right bottom and left top are compressed)-Fig. 6a.

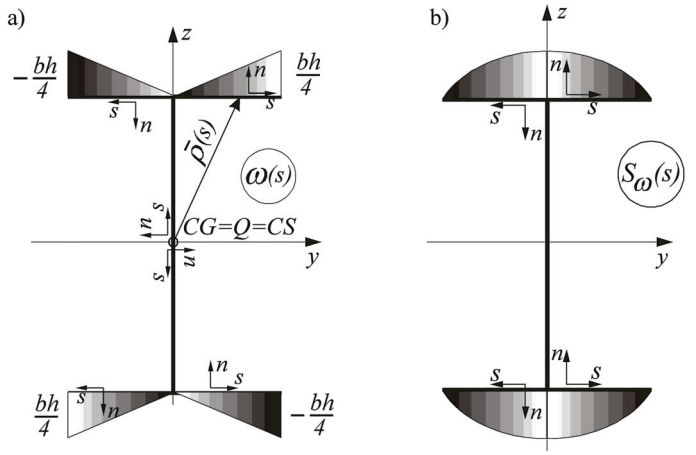

Fig. 5. Plots of: a) sectorial co-ordinate, b) sectorial static moment, for bisymmetric I-section

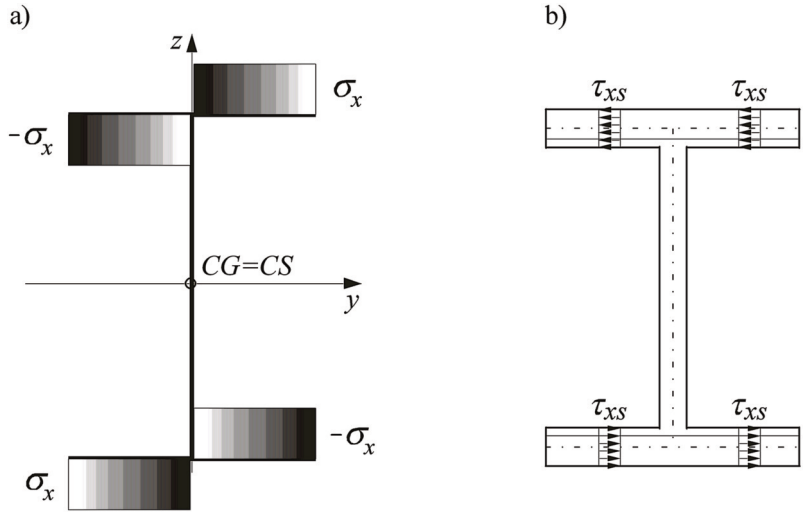

Fig.6. Diagrams of stresses in plastic hinge, predicted in accordance with the Vlasov theory: a)normal, b) shear, for twisted cantilever I-section thin-walled beam

The ordinate of stresses is not equal to the magnitude of σ_Y, because the plastic state is also generated by shear component of the stress tensor. Because only M_ω exists (M_s=0), the value τ_{xs} should be constant over the cross-section thickness and should be determined by $S_{\omega(s)}$ only. Let us consider the right top part of the cross-section-Fig. 5b.

The sectorial static moment diagram is placed on positive side of n-axis in the local co-ordinate system, which implies that the $S_{\omega(s)}$ values are positive for this location. The M_ω magnitude is also positive-Fig. 3b, so in accordance with formula (7) the shear stresses at right top part of section should be negative. The appropriate distribution is depicted in Fig. 6b-the shear stresses at analysed parts of the top flange are negative, because they have the opposite direction to *s*-axis in the local co-ordinate system. Basing on the presented algorithm the remaining distributions can be found-Fig. 6b. The shear stress value can be taken as constant for all points of flanges, because in plastic hinge (in the full plastic state) it is related to constant σ_x by equation (4), at each point.

That the assumed normal stresses distribution is correct, was confirmed by FEM limit state simulations. Fig. 7 shows a map of σ_x for beam middle surface near the fixed end of I-section twisted profile, obtained utilising shell elements.

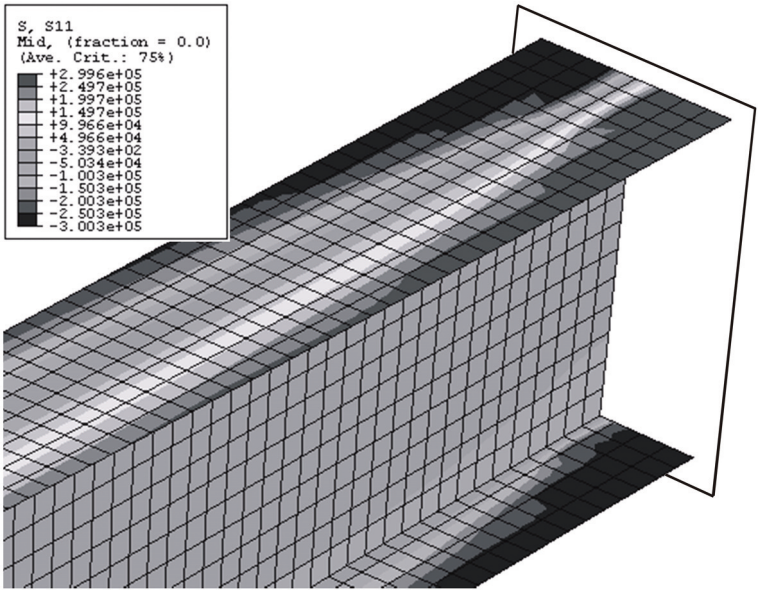

Fig. 7. Normal stress distribution in a plastic hinge obtained by FEM (program Abaqus) - twisted I-section cantilever profile - middle surface

The predicted diagram - Fig. 6a is the same as this which bases on computation data, that implies that stress distributions in plastic hinge can be based on the Vlasov theory.

3. BENDING WITH TORSION OF I-SECTION THIN-WALLED BEAM

This case is often encountered in engineering practice. For example, such situation is recalled in Fig. 8.

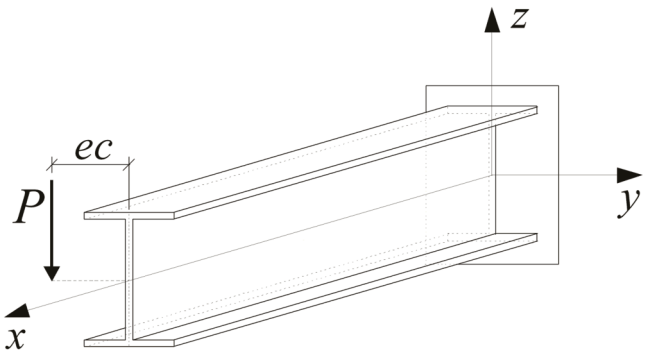

Fig. 8. The case of bent and twisted I-section cantilever thin-walled beam

Five cross-sectional forces will appear in this case. The distributions of the three of these along the beam length: bimoment, the Vlasov torsional moment and the Saint-Venant torsional

moment, follow the same pattern as in the previous example - Fig. 3. The remaining stress resultants: bending moment M_y and shear force F_z are well-known from solid beams theory.

The first varies linearly from zero at the free end of profile to the maximum value for $x = 0$, whereas shear force diagram is constant. It is readily apparent that the occurrence of bending in the torsion case - Fig. 3, does not change the most exerted cross-section locus.

Hence the plastic hinge is again placed at the fixed end of the beam. The fact that M_y and F_z exist, prompts us to develop stress limit diagrams using the following formulas:

$$\sigma_x(s) = \frac{B_\omega}{I_\omega}\omega(s) + \frac{M_y}{I_y}z(s) \tag{8}$$

$$\tau_\omega(s) = -\frac{M_\omega S_\omega(s)}{I_\omega \delta} + \frac{F_z S_y(s)}{I_y \delta} \tag{9}$$

The diagrams of new functions, which determine stress distributions in elastic state, are shown in Fig. 9.

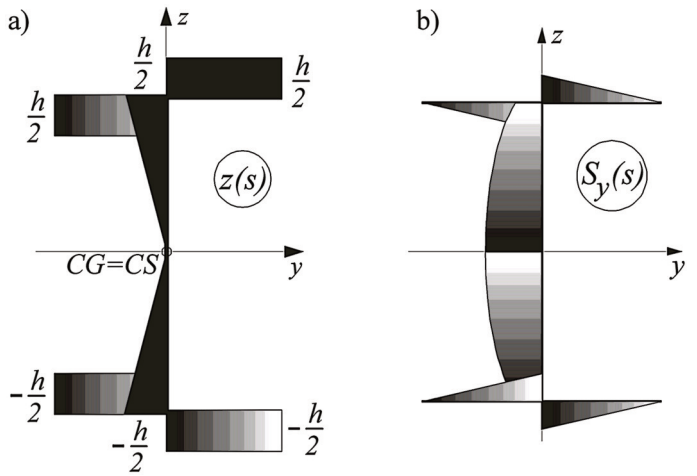

Fig. 9. The diagrams of: a) z co-ordinate, b) static moment with respect to y-axis, for bisymmetric I-section

Fig. 9a shows that the asymmetric normal stresses diagram - Fig 6a, valid for torsion, will be disturbed by a constant positive σ_x values in the top flange case and by constant negative quantities in the bottom flange case. That implies that tension should prevail over compression when the top flange is considered, whereas the reversed situation holds for the bottom flange.

Combining the two diagrams - Fig. 5a and Fig. 9a leads to relocation of neutral points σ_x distributions in flanges - Fig. 6a.

Additionally, normal stress due to bending in profile web suggests that limit diagram presented in Fig. 10a would be correct. The parameter u depends on the B_ω/M_y ratio. The magnitude σ_x is not equal to the tensile yield stress value, because shear stresses also exist.

The distribution of τ_{xs} in flanges - Fig. 10b, is related to M_ω (for typical cross-section sizes encountered in practical applications the influence of shear force can be neglected). It appears that the τ_{xs} diagram for flanges is the same as in torsion - Fig. 6b and Fig. 10b.

The nonzero value of F_z causes the shear stresses to appear in web. For the analysed loading example - Fig. 8, the magnitude of shear force is negative (the remaining cross-sectional forces

are positive). In accordance with equation (9) the sign of the shear stress must be opposite to that of the static moment $S_y(s)$. In the upper half of the web the $S_y(s)$ values are positive whereas in the lower - negative. A thorough analysis of the local co-ordinate systems-Fig. 5a reveals the τ_{xs} distribution should be taken as constant for the entire web-Fig. 10b. The magnitudes of σ_x and τ_{xs} must satisfy formula (4), which guarantees the plastic state in each point of cross-section.

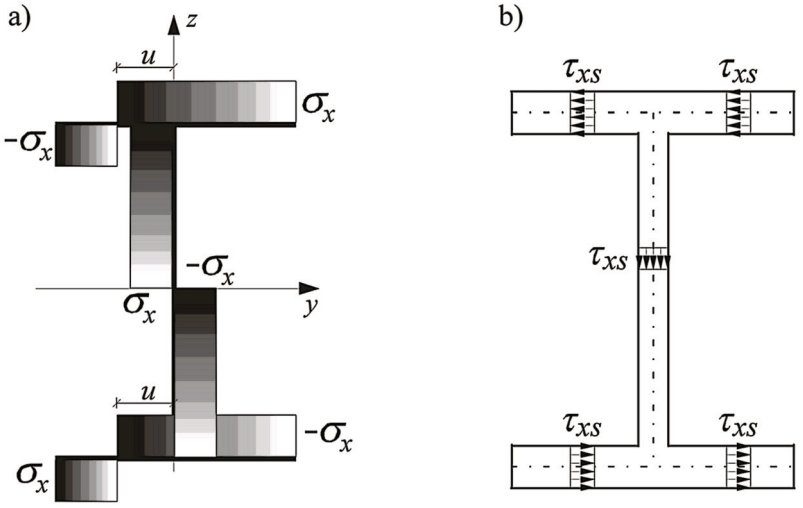

Fig. 10. The distributions of: a) normal stresses, b) shear stresses, in a plastic hinge, for bent and twisted cantilever I-section of a thin-walled beam (in accordance with the Vlasov theory)

The adequacy of the assumed diagram-Fig. 10a, is confirmed by the shell element analysis (Abaqus). The task in Fig. 8 was modelled and all relevant conditions (boundary, load, etc.) duly accounted for. FEM calculations were applied in simulations of the experiment described in [5]. The value of force applied to the computational model of a beam is equal to the load capacity at collapse obtained from Strelbicka et al. and hence the limit state simulation is performed.

The distributions depicted in Fig. 10a and Fig. 11 are very similar, which is a proof that the Vlasov theory can be employed to construct limit stress diagrams in the thin-walled beams case.

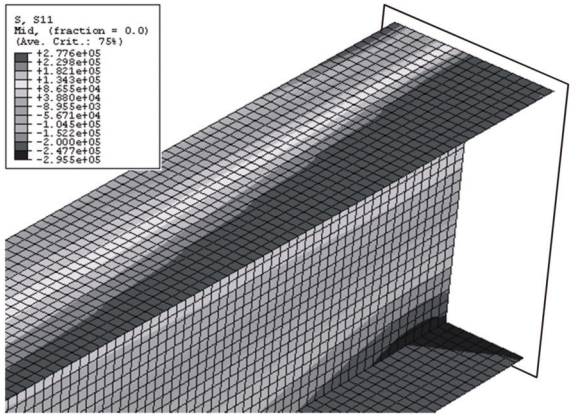

Fig. 11. Normal stress distribution in a plastic hinge obtained by FEM (program Abaqus) -bent and twisted I-section cantilever profile-middle surface

4. ALGORITHM OF DETERMINATION OF LOAD CAPACITY AT COLLAPSE-CALCULATION PROCEDURE IN THE CASE OF THIN-WALLED BEAMS

Predicted diagrams of stresses in plastic hinge can be utilised to formulate the analytic approach, which enables the assessment of load capacity at collapse of thin-walled beams with open cross-sections. Study presented below is the outline of this method for bent and twisted I-section cantilever profiles. Let us consider the general case all cross-sectional forces are non-zero. Accordingly, diagram in Fig. 10a can be well used. In Fig. 10b, however, the influence of the Saint-Venant moment should be taken into account. For positive M_S (when only the Saint-Venant moment exist) the limit stress distribution for any cross-section leg is shown in Fig. 12a.

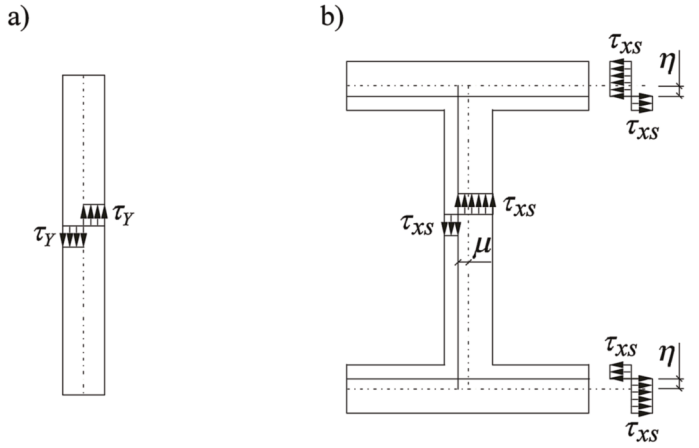

Fig. 12. The limit shear stress distributions: a) generated only by M_S moment for a single cross-section leg, b) generated by M_S, M_ω and F_Z stress resultants for I-section in the case of beam bending and torsion

The assumed shear stresses must be oriented counter-clockwise. If this diagram is taken into account in Fig. 10b for each cross-section leg, we obtain the distribution given in Fig. 12b. The diagram in the web-Fig. 10b must be re-constructed, because only positive stress resultants can be considered.

The results of study are distributions shown in Fig. 10a and Fig. 12b. The application of predicted diagrams in the derivation of interaction surface formula is illustrated by an algorithm in Fig. 13.

The considered stresses distributions are utilised to develop equivalence relationships, given in general form by expressions (10)-(14).

$$B_\omega = \int_d \sigma_x(s)\omega(s)\delta(s)\mathrm{d}s \tag{10}$$

$$M_y = \int_d \sigma_x(s)z(s)\delta(s)\mathrm{d}s \tag{11}$$

$$M_\omega = -\iint_A \tau_{xs}(s,n)\rho_n(s)\mathrm{d}A \tag{12}$$

$$M_s = -2\iint_A \tau_{xs}(s,n)n\mathrm{d}A \tag{13}$$

$$F_z = \iint_A \tau_{xs}(s,n)\dot{z}(s)\mathrm{d}A \tag{14}$$

The equation (14) contains the derivative with respect to s. Application of equations (10)-(14) in the case shown in Fig. 10a and Fig. 12b leads to the formulae expressing the dependence of cross-sectional forces on parameters: *u, η, μ.*

When these parameters are reduced, we derive algebraic equations governing normal σx and shear τ_{xs} stresses in plastic hinge-Fig. 13.

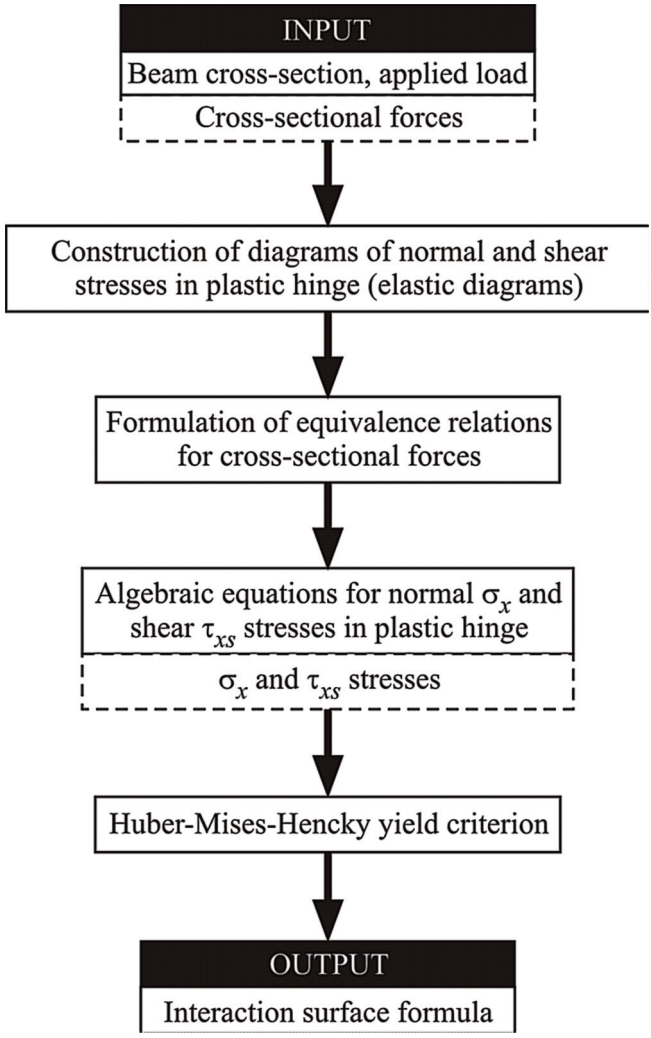

Fig. 13. The algorithm for deriving the interaction surface formulae

After solving the algebraic expressions, the calculated limit stresses are substituted to condition (4), which completes the derivation of the interaction surface formula (15).

$$
\begin{aligned}
&2\left[\frac{B_\omega(x_o)-T_1M_y(x_o)}{T_2\sigma_Y}\right]^2+\frac{M_y^2(x_o)}{T_3\sigma_Y^2}+\\
&+2\frac{B_\omega(x_o)-T_1M_y(x_o)}{T_2\sigma_Y^2}\sqrt{\frac{\left[B_\omega(x_o)-T_1M_y(x_o)\right]^2}{T_2^2}+\frac{M_y^2(x_o)}{T_3}}+\\
&+\frac{M_s^2(x_o)}{2M_{sY}^2}+\frac{1}{M_{sY}\tau_Y}\left[\frac{F_z^2(x_o)}{2h}+\frac{M_\omega^2(x_o)}{bh^2}\right]+\\
&+\frac{M_s(x_o)}{M_{sY}\tau_Y}\sqrt{\frac{M_s^2(x_o)}{4T_4^2}+\frac{1}{T_4}\left[\frac{F_z^2(x_o)}{2h}+\frac{M_\omega^2(x_o)}{bh^2}\right]}=1
\end{aligned}
\tag{15}
$$

where:

$$
T_1=\frac{h\delta_w}{8\delta_f},\ T_2=\frac{hb^2\delta_f}{2}-\frac{h^3\delta_w^2}{32\delta_f},\ T_3=h^2b^2\delta_f^2-\frac{h^4\delta_w^2}{16},\ T_4=h\frac{\delta_w^2}{2}+b\delta_f^2,
$$

$$
M_{sY}=\frac{\sigma_Y}{\sqrt{3}}T_4=\tau_Y\left(h\frac{\delta_w^2}{2}+b\delta_f^2\right)
$$

x_o-abscissa of cross-section with a plastic hinge,
h-height of I-section (measured between middle lines of flanges), b - width of flanges,
δ_w-thickness of web, δ_f - thickness of flanges

This equation will be used for calculation of load capacity at collapse, in an example presented in Fig. 8. Numerical data are summarised below:

h=114 mm, b=74 mm, δw=5 mm, δf=6 mm, beam length-L=1.275 m, material constants-E =210 GPa, v = 0.3, σY =254.7 MPa, force eccentric-ec =6 cm.

The plastic hinge appears at the fixed end of the beam (xo = 0). The cross-section effort is determined by values of stress resultants. The cross-sectional forces are obtained from expressions (5) after solving a differential equation (3).

In this case boundary conditions for (3) are:

$$
\alpha(0)=0,\ \alpha'(0)=0 \text{ -warping restraint, } \alpha''(L)=0 \text{ -absence of bimoment} \tag{16}
$$

The magnitudes of stress resultants for x_o=0 are: B_ω=0.02944P, M_y=1.275P, M_ω=0.06P, M_s=0, F_z=-P. In these relationships the [m] and [kN] units are valid.

Substituting the values of cross-sectional forces to formula (15), the limit magnitude of force P (the load capacity at collapse) is calculated. For considered numerical data the desired value is given in Table 1 - first column.

Tab 1. The set of load capacity at collapse values for I-section cantilever profile subjected to bending and torsion

Based on the Vlasov thin-walled beams theory	Based on the Vlasov theory (taking into account the normal stresses only)	Comparison of values from first and second column	Based on experimental data from [5]	Comparison of values from first and fourth column
[kN]	[kN]	[%]	[kN]	[%]
6.976	6.992	0.2294	7.6	8.9

Whether bimoment and bending moment (stress resultants related to σ_x) are of major importance is checked by calculation of load capacity at collapse for the case when the remaining nonzero cross-sectional forces: M_ω, F_z are assumed to be zero. The result is shown in the second column of Table 1. The difference is very small-the third column of Table 1, hence in similar situations (when a plastic hinge appears in the place where cross-sectional forces related to normal stresses have extreme magnitudes and where the Saint-Venant torsional moment is equal zero) the influence of τ_{xs} on load capacity at collapse value can be omitted.

The example considered in this study was investigated by Strelbicka et al.-[5]. The discrepancy between the tensile yield stresses of web and flanges materials was simulated in an analytic approach by using of one weighted value (the web and flanges moments of inertia with respect to *y*-axis had weight factors). The result of experiment is given in fourth column-Table 1. The load capacity at collapse is larger than that obtained analytically.

The method based on the Vlasov theory gives a more conservative assessment limit force, which is a major advantage. Furthermore, the level of difference (set in the last column of Table 1) is acceptable. A certain underestimation is also confirmed by FEM analysis whereby load equal to the limit value (column 1 Table 1) is applied to the beam model. The distribution of equivalent plastic strains (the plastic zone range) is illustrated by Fig. 14..

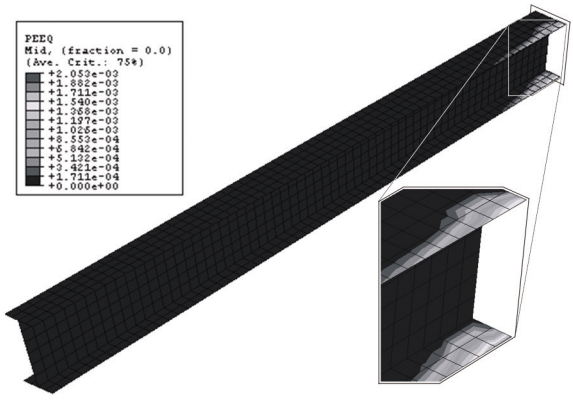

Fig. 14. The equivalent plastic strains distribution for bent and twisted I-section cantilever profile (Abaqus) - middle surface

The plastic yield areas do not spread over the entire cross-section, so indeed the load value derived analytically will remain below load capacity at collapse.

The analytic, experimental and computational data display a high degree of correspondence, which confirms the accuracy of results obtained by a method based on the Vlasov theory.

5. THE „MONITORING AREAS" APPROACH

Let us consider FEM simulations of limit state of a thin-walled cantilever channel beam - Fig. 15. The load applied to a profile model is the same as in Fig. 8. Fig. 15a shows the normal stress distribution near the fixed end of the beam (where a plastic hinge appears) over the middle surface, Fig. 15b provides the same map for a boundary exterior layer (surface of profile).

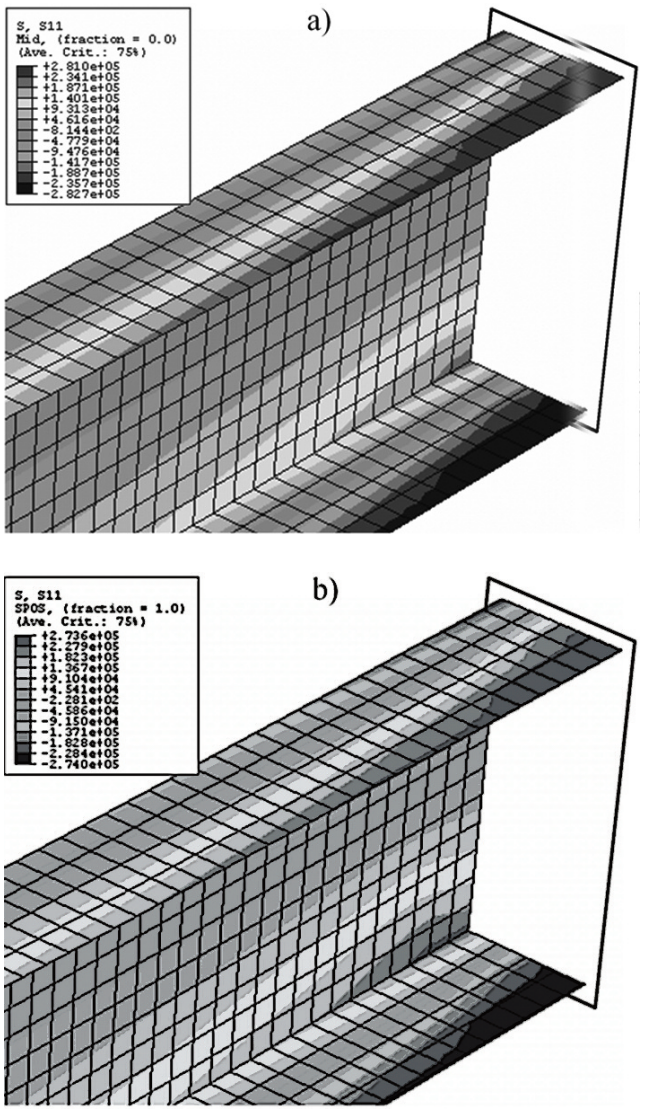

Fig. 15. The limit distributions of normal stresses: a) for middle surface, b) for boundary (exterior) surface, at fixed end (in plastic hinge) of bent end twisted cantilever channel profile

The tensile yield stress of the analysed material approaches 240000 kPa. Fig. 15 reveals that normal stresses in a plastic hinge are nearing σ_Y. These stress magnitudes are represented by the first and the last ranges at maps legends - Fig. 15. It is reasonable to suppose, recalling equation (4), that values of shear stresses in plastic hinge are very small (and do not approach the shear yield stress τ_Y). Hence in the limit state the distributions of τ_{xs} are the same as in the elastic range. That is why predicted diagrams of elastic shear stress (linearly variable along the profile thickness) in a plastic hinge better portrays the analysed situation.

For a cantilever thin-walled channel beam, subjected the load shown in Fig. 8, the relevant distributions are shown in Fig. 16a and Fig. 16b.

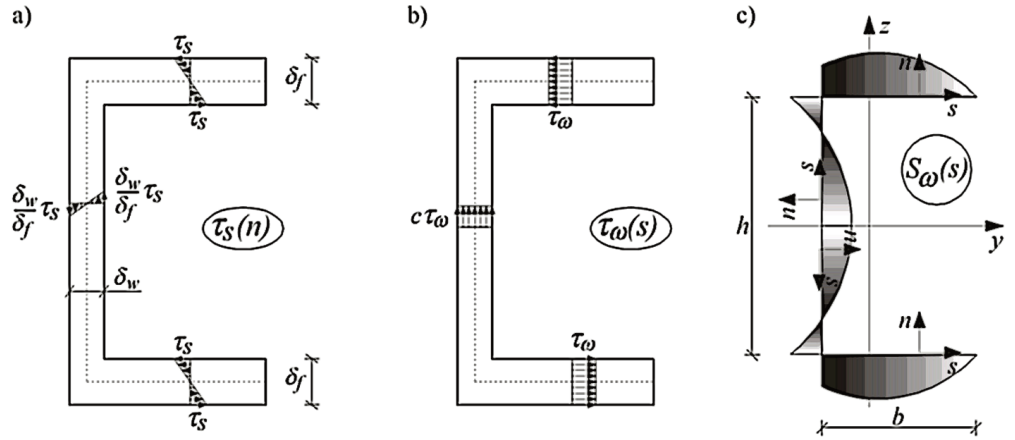

Fig. 16. The diagrams of: a) elastic shear stresses related to Ms, b) elastic shear stresses related to M_ω and *Fz*, c) sectorial static moment, for channel profile in the case of bending and torsion

The first diagram-Fig. 16a, applies to a positive M_S. This plot is characteristic of the Saint-Venant torsion. The second diagram-Fig. 16b, gives the Vlasov torsional moment M_ω and shear force F_Z. The distributions in flanges are related with the two cross-sectional forces.

In accordance with formula (9), the positive $S_\omega(s)$-Fig. 16c, in upper flange produces (for positive M_ω) the negative stresses (opposite to *s*-axis-Fig. 16c).

In the case of a lower flange, we get the reverse situation. The influence of *Fz* in flanges reveals the same features as M_ω. In the web, however, shear force prevails over the Vlasov torsional moment work, so diagram with a constant turn (characterised of F_z) can be assumed. The stresses are directed from bottom to top-Fig. 16b, as it was the case of the positive shear force. The parameter *c* determines the difference between the web and flanges distributions. Stress plots in Fig 16 do not vary along the length of profile legs, because they are basis for the analytic method (enabling the assessment of load capacity at collapse) and therefore should not be too complicated.

In the plastic hinge the condition (4) must be fulfilled at each point of the cross-section. A diagram of normal stresses in limit state linearly variable through the profile thickness would be required, which complicates the problem. The good solution is provided by the „monitoring areas" idea. Accordingly, the entire cross-section is divided into layers - Fig. 17a.

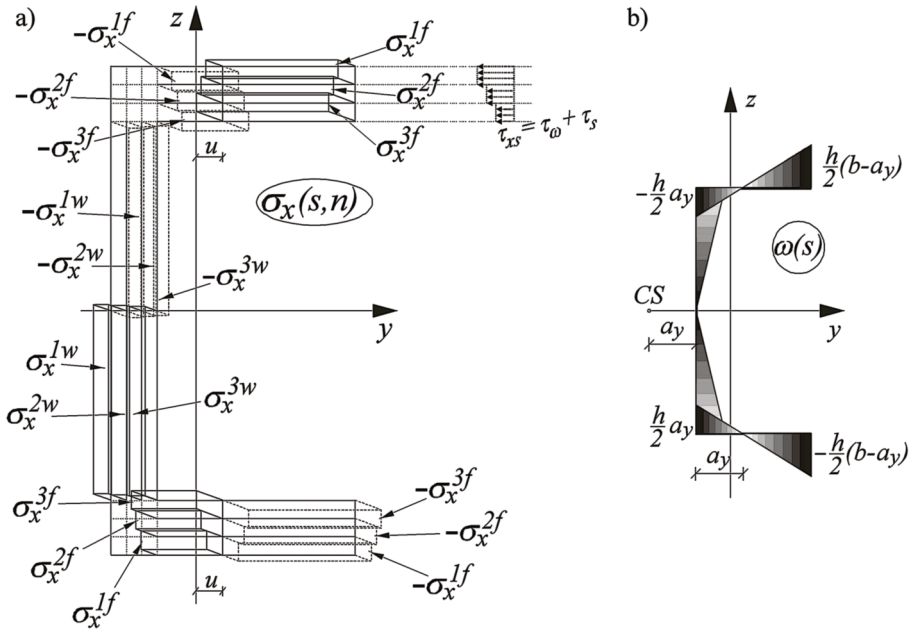

Fig. 17. The diagrams of: a) normal stresses in plastic hinge for bending and torsion - in accordance with „monitoring areas" approach, b) sectorial co-ordinate, in the case of thin-walled channel beam. The application of the „monitoring areas" approach to the investigation of shear stresses indicated with dot line

The linear shear stress diagrams are substituted by stepped diagrams - Fig. 17a - dot line, similar to normal stress distributions. For each layer the values of σ_x and τ_{xs} are constant. The number of used layers depends on the desired accuracy of load capacity at collapse calculations. In accordance with equation (4), it is required that the greatest value of τ_{xs} in the exterior layer be accompanied by the smallest σ_x at the same place.

This explains the normal stress distributions through the cross-section thickness.

Instead, the σ_x distribution along the length of cross-section legs is determined by *ω(s)* and *z(s)* functions, as revealed by equation (8). When torsion plays the key role, the sectorial co-ordinate diagram prevails over *z(s)* co-ordinate and the distribution shown in Fig. 17b is decisive. So, the diagram presented by Fig. 17a describes normal stresses distribution in plastic hinge where load eccentricity *ec* is large.

The characteristic phenomenon occurs when eccentricity *ec* is slightly larger than distance a_y -Fig. 17b. The impacts of positive B_ω and M_y are equal. The first cross-sectional force is related to negative linear σ_x diagram in the upper half of the web-Fig. 17b, whereas the positive bending moment generates the positive linear normal stress distributions (well-known from the solid beams theory) at an analysed place. The loading process is responsible for the balance effect in both σ_x diagrams at the web. This „non-loading" of the web must be taken into account when constructing the normal stress distribution in a plastic hinge for the given case.

The predicted diagram of σ_x for the limit state (when torsion (B_ω) dominates)-Fig. 17a, is confirmed by FEM (Abaqus) simulations - Fig. 15. The distributions along middle line and through the cross-section thickness obtained analytically and by computation procedure are the same. The greater values of normal stresses in middle surfaces of flanges (when compared to exterior layers) are presented by the first and last areas in the map legends - Fig. 15. In the web,

the stress distribution through the cross-section thickness (Fig. 17a) is reverse to that illustrated in Fig. 15, because the directions of shear force in these two cases are opposite.

Limit stress diagrams shown in Fig. 16a, Fig. 16b and Fig. 17a can be utilised to derive interaction surface formula, which enables the assessment of load capacity at collapse. The algorithm is similar to that presented in Fig. 13. However, the normal and shear stress states are not analysed simultaneously, first we consider τ_{xs} and next the yield condition (4)is formulated for each layer separately. Finally, the σ_x problem (with normal stress magnitudes calculated in the two previous steps) is investigated.

The analytic approach to finding load capacity of thin-walled beams at collapse, based on „monitoring areas" approach, is particularly useful in the study of cases where the Saint-Venant torsional moment (τ_{xs}) has major influence in limit state creation.

6. CONCLUSIONS

It is shown that the Vlasov theory can be well used for building the normal and shear stress diagrams in plastic hinge for thin-walled beams and evaluating profiles exertions. Basing on elastic stress distributions (consistent with sectorial co-ordinates and sectorial static moments functions), the virtual expansion of yield zones leads to creation of proper limit stresses diagrams. The FEM (Abaqus) simulation confirms the adequacy of predicted plastic hinges shapes. The computation data indicate that evaluation of thin-walled beam exertion (i.e. finding of the plastic hinge locus) through the analysis of cross-sectional forces diagrams (developed in accordance with the Vlasov theory) produces good results. Limit stress diagrams developed in this study can be utilised to formulate interaction surface formulae, which enable assessment of load capacity at collapse in the case of thin-walled beams.

The constructed analytic method affords us the thesis that we obtain the underestimated values of limit load, which is verified by experimental and calculation data. It is reasonable to suppose that this approach can be used in design, because provides safe values of load capacity at collapse. This method can be also treated as a tool for verification of new algorithms (algorithms for determination of limit load). It appears that in the cases when the Saint-Venant torsional moment does not contribute to the formation of a plastic hinge, the influence of shear stresses on the limit load can be omitted. Conversely, when shear stresses are not negligible, the „monitoring areas" approach should be adopted to calculate more exact values of load capacity at collapse.

Acknowledgments

The author would like to express his gratitude to Professors Stefan Piechnik and Ryszard B. Pęcherski for their permanent interest and many valuable suggestions during the work on this subject.

BIBLIOGRAPHY

[1] Vlasov WZ. Thin-walled elastic beams [in Russian]. Moscow: State Publishers of Physical and Mathematical Literature, 1959.
[2] Piechnik S. Thin-walled beams with open cross-sections [in Polish]. Krakow: Krakow University of Technology, 2000.
[3] Życzkowski M. Combined loadings in the theory of plasticity. Warsaw: PWN - Polish Scientific Publishers, 1981.

[4] Strelbicka AI. Investigation of the strength of thin-walled beams beyond the elastic limit [in Russian]. Kiev: Academy of Science, Ukrainian S.S.R., 1958.
[5] Strelbicka AI, Jewsiejenko GI. Experimental investigation of elastic-plastic behaviour of thin-walled structures [in Russian]. Kiev: Publishers „Naukowa Dumka", 1968.
[6] Gawłowski S, Pęcherski RB. Analysis of load-capacity at collapse of I-section thin-walled beam. Engineering Transactions 2004;52(1-2):5-22.
[7] Gawłowski S, Pęcherski RB. Static assessment of load capacity at collapse of open cross-section thin-walled beams. Shell Structures: Theory and Applications -Pietraszkiewicz & Szymczak (eds), A.A. Balkema Publishers 2005. London: Taylor & Francis Group:219-223.
[8] Abaqus (standard). Reference manuals ver. 6. 4-1. Providence: Hibbitt, Karlsson & Sorensen, Inc., 2004.
[9] Orkisz J. Limit curves for replacement multi-point cross-sections of beams under elastic-plastic bending [in Polish]. Technical Journal 1962;52(6):1-11.
[10] Izzuddin BA, Lloyd Smith D. Large-displacement analysis of elastoplastic thin-walled frames. Journal of Structural Engineering 1996;122(8):905-925.

SEBASTIAN GAWŁOWSKI

ANALIZA STATYCZNA STANU GRANICZNEGO PLASTYCZNEGO PRĘTÓW CIENKOŚCIENNYCH O PRZEKROJACH OTWARTYCH

Streszczenie

Praca przedstawia implementację teorii Własowa do opisu własności prętów cienkościennych otwartych w stanie granicznym plastycznym. W szczególności zajęto się konstruowaniem rozkładów naprężeń normalnych i stycznych w przegubach plastycznych. Rozważania pokazują, iż teoria Własowa stanowi idealne narzędzie do przypuszczania granicznych plastycznych rozkładów naprężeń w przypadku rozpatrywanej grupy profili. Rozwinięciem analizy jest skonstruowanie podejścia analitycznego służącego szacowaniu nośności granicznej prętów cienkościennych otwartych. Ilustracją rozważań są znane z praktyki inżynierskiej przykłady liczbowe obejmujące zginanie i skręcanie profili dwuteowych oraz ceowych. Poprawność otrzymanych wyników analitycznych jest potwierdzona przez przytoczone rezultaty obliczeń numerycznych MES jak i dostępne dane doświadczalne. Na zakończenie zaprezentowano ideę „monitorowanych pól", która pozwala na precyzyjniejszy opis zachowania się prętów cienkościennych otwartych w stanie granicznym plastycznym.